Journal of Energy

VOLUME 64 Number 1–4 | 2015 Special Issue

journal homepage: http://journalofenergy.com/

SINIŠA ŠADEK **DAVOR GRGIĆ**

sinisa.sadek@fer.hr davor.grgic@fer.hr

University of Zagreb Faculty of Electrical Engineering and Computing

NPP KRŠKO CONTAINMENT MODELLING WITH THE ASTEC CODE

SUMMARY

ASTEC is an integral computer code jointly developed by *Institut de Radioprotection et de Sûreté Nucléaire* (IRSN, France) and *Gesellschaft für Anlagen- und Reaktorsicherheit* (GRS, Germany) to assess nuclear power plant behaviour during a severe accident (SA). The ASTEC code was used to model and to simulate NPP behaviour during a postulated station blackout accident in the NPP Krško. The accident analysis was focused on containment behaviour; however the complete integral NPP analysis was carried out in order to provide correct boundary conditions for the containment calculation. During the accident, the containment integrity was challenged by release of reactor system coolant through degraded coolant pump seals, molten corium concrete interaction and direct containment heating mechanisms. Impact of those processes on relevant containment parameters, such as compartments pressures and temperatures, is going to be discussed in the paper.

Key words: ASTEC, core melt, direct containment heating, molten corium concrete interaction, PWR

https://doi.org/10.37798/2015641-4150

1. INTRODUCTION

Release of radioactive material into the environment is a major concern during a hypothetical severe accident. A last barrier for a radioactive release in a pressurized water reactor (PWR) nuclear power plant (NPP) is the containment, a reinforced concrete structure which encloses main components of the primary cooling circuit. Since the containment has a large interior volume, it cannot withstand a significant pressure difference between the inner and the outer surfaces. Failure of a reactor pressure vessel (RPV) and discharge of a core melt may challenge the containment integrity.

A station blackout accident combined with a small LOCA following degradation of reactor coolant pump (RCP) seals was chosen as a reference severe accident (SA) event. The loss of coolant from the reactor cooling system (RCS) and unavailability of safety injection (SI) systems will lead to core uncover, heat-up and, finally, degradation and melting. Formation of an in-core molten pool and its slumping to the RPV lower head may cause failure of the RPV bottom wall due to increased thermal and mechanical stresses. The released corium accumulates at the concrete bottom of the reactor cavity. Molten corium concrete interaction (MCCI), which begins after the corium hits the cavity bottom, is accompanied with release of hydrogen and carbon monoxide which are flammable and explosive gases. Inert gas CO_2 is also produced and, although it does not represent an explosion hazard, its rather high production rate will be the main contribution factor to the containment pressure increase. Beside the MCCI, another phenomenon called direct containment heating (DCH) will be responsible for the containment pressurization and heat-up. In the case of the DCH, molten debris is dispersed in the containment atmosphere where the decay heat of the melt is transferred to containment structures and walls, and also to air and steam. With increase of the amount of the corium discharged during the DCH, the effects of the MCCI will be less severe; however accumulation of gases in the containment can lead to substantial pressure increase rate. Containment integrity, thus, can be more seriously challenged during the DCH than the MCCI.

The ASTEC code version ASTEC-V2.0-rev3p1 was used in the calculations. The ASTEC is a modular computer code consisting of 13 coupled modules that model different SA phenomena. For the purpose of presented analyses eight modules were used: CESAR, ICARE, CPA, MEDICIS, RUPUICUV, CORIUM, COVI and SYSINT. The CESAR module computes two-phase thermal hydraulics (TH) in the primary and secondary circuits. Modelling is based on a 1D, two-fluid, five-equation approach. One incondensable gas (hydrogen) is available. The ICARE module models in-vessel core degradation and vessel rupture [1]. The thermal hydraulics in the core is based on a 1D swollen water level approach completed by a 2D gas modelling. The corium behaviour in the lower plenum is based on a 0D modelling of corium layers (oxide, metallic and debris layers) with a 2D meshing of the RPV lower head. The molten corium concrete interaction is simulated by the MEDICIS module [2]. Direct containment heating generated by discharge of corium after the vessel rupture is modelled by the RUPUICUV module [3] and the behaviour of corium droplets transported by high pressure melt ejection into the containment atmosphere and the sump by the CORIUM module [4]. Inside the containment the CPA module is responsible for the thermal hydraulic and aerosols behaviour calculation and the COVI module for the hydrogen build-up (a simple model assuming a virtual combustion, i.e. an adiabatic total combustion without any feedback on the CPA thermal hydraulics). For the H_2 and CO combustion analysis in the containment, a more detailed model (the so-called CPA-FRONT) exists in the ASTEC-V2 but it was not used here. The SYSINT module manages all engineered safety features such as spray actuation, the safety injection system, accumulator injection, pump operation, etc.

Other five modules are ELSA, SOPHAEROS, ISODOP, IODE and DOSE. The ELSA module takes care of fission products and structural material release from the core, while their transport in the RCS is modelled by the SOPHAEROS module. The ISODOP module calculates the fission products and actinide isotope decay, the IODE module the iodine chemistry and the DOSE module, dose rates in different containment compartments.

2. MATHEMATICAL MODEL OF THE NUCLEAR POWER PLANT

The NPP Krško mathematical model includes detailed models of primary and secondary systems, Figure 1, and the containment, Figure 2. The reactor coolant system, steam generators (SG), steam lines, feedwater and auxiliary feedwater (AFW) pipes are modelled as a set of thermal hydraulic volumes connected by junctions, to which heat structures were attached to simulate heat losses to the environment. The ICARE module is used to model the reactor core and the CESAR module to model all other plant systems: primary and secondary circuit pipings, the pressurizer and the steam generators. Heat losses from the primary system to the containment are modelled with the substructure HEAT from the CONNECTION structure.

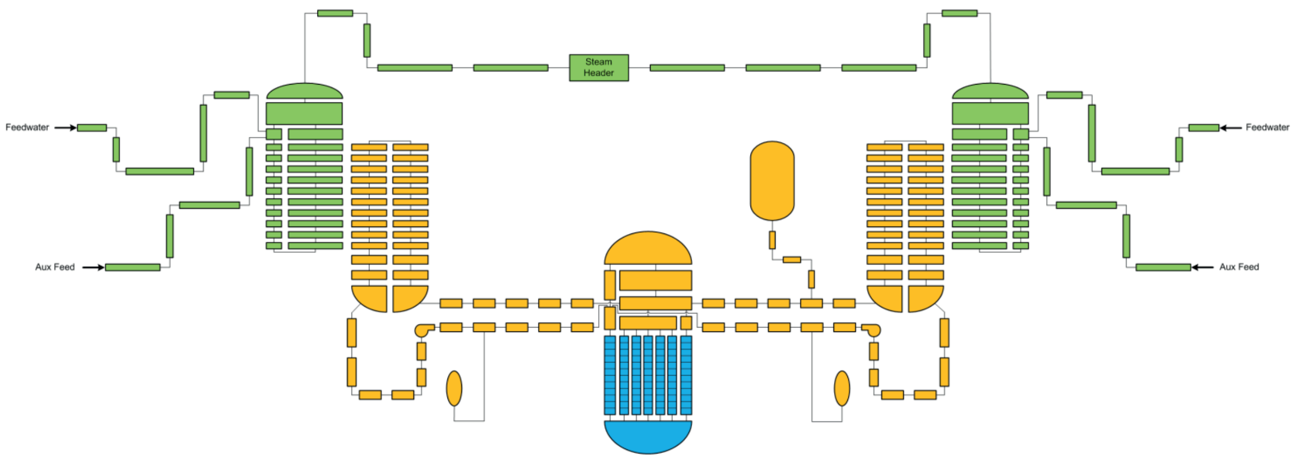

Figure 1. Primary and secondary systems nodalization for the ASTEC calculation

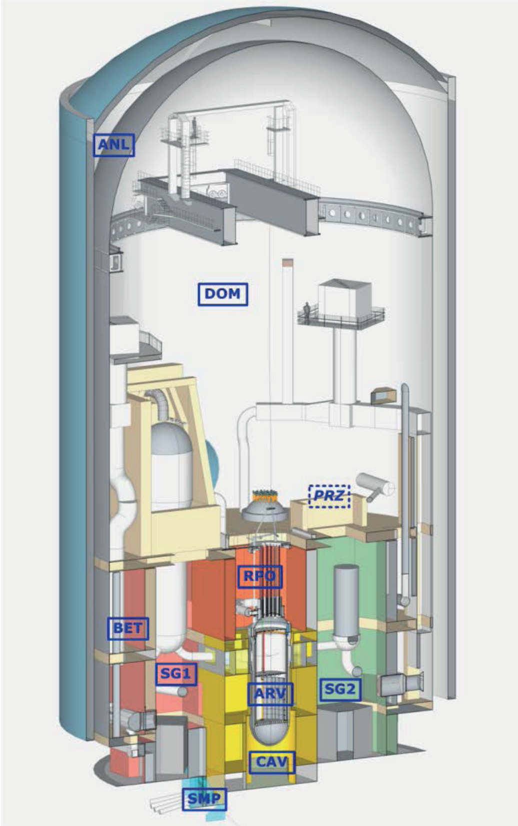

Figure 2. Containment 3D nodalization sketch for the ASTEC calculation

The containment building is represented with 10 control volumes:

1. DOM (containment dome) – cylindrical/spherical air space above the reactor pool, steam generators and pressurizer compartments,
2. ANL (annulus) – air space between the steel liner and the containment building,
3. SG1 (steam generator 1 compartment) – air space in the SG1 compartment that contains components SG1 and RCP1,
4. SG2 (steam generator 2 compartment) – air space in the SG2 compartment that contains components SG2 and RCP2,
5. PRZ (pressurizer compartment) – air space in the compartment that contains pressurizer and primary system safety and relief valves,
6. BET (between) – lower compartment below the containment dome placed between SG1, SG2 and PRZ compartments excluding the reactor pool and the reactor pressure vessel area,
7. RPO (reactor pool) – air space above the reactor vessel filled with water during the shutdown, otherwise empty,
8. ARV (around reactor vessel) – air space between the reactor vessel and the primary shield walls,
9. CAV (reactor cavity) – air space below the reactor vessel including the instrumentation tunnel,
10. SMP (containment sump) – the lowest control volume below the SG1 compartment that contains the recirculation sump.

An additional control volume with a large volume and fixed temperature (35 °C) is used to represent the environment. This volume is necessary for the code to calculate heat losses from the containment building. Heat transfer coefficient from the outside containment wall to the environment is calculated by the code.

The control volumes are connected with 23 junctions. That number of junctions is larger than required just to connect simply the volumes. More than one opening is used between the same volumes if they are located at different elevations to promote internal thermal mixing flow, what can be important for long term containment transients. For example, there are three connections between the BET volume and SG1 and SG2 compartments, respectively, at floor levels. There are also more than one connection between the DOM volume and volumes SG1, SG2 and PRZ. Pressurizer and steam generator compartments are open and the junction areas between those compartments and the dome are large, between 6 m^2 and 35 m^2. Other connections, such as between ARV and SG1 and SG2 compartments which are through cold and hot leg openings in the primary shield wall are smaller; their values were taken to be 1 m^2. Connection between the sump and the cavity is based on cross section area of 4 inch pipe. The largest connection area is between the reactor pool and the dome, 108 m^2. The sump and the cavity are connected to the SG1 compartment and the BET volume, respectively. The reactor sump is below the SG1 compartment with the connection area being 4.5 m^2. The cavity is indirectly connected to the lower containment compartment (BET) through the water tight door. Depending on the state of that door, two cavity types might develop, the "wet cavity" and the "dry cavity", depending on the possibility of water flow from the lower compartment to the cavity. Both cases were analyzed and discussed in the next section.

Heat sinks are represented with 79 heat structures. The steel liner, the containment building wall, internal concrete and steel walls and floors are explicitly modelled. Five heat structures are used to model the steel liner and the containment wall. Internal walls and structures, such as the polar crane and fan coolers, are represented with 66 heat structures. Floors at three different elevations are represented with three heat structures. The last five heat structures represent the bottom concrete floor. The heat transfer coefficients for convective heat exchange between TH volumes and structures are calculated internally by the code. Total convective heat transfer areas are as follows:

1. Steel liner – 5950 m2
2. Containment building concrete wall – 6940 m2
3. Internal walls and structures
    a. Concrete – 2940 m2
    b. Steel (stainless and carbon steel) – 31150 m2
4. Floors (concrete) – 1560 m2
5. Bottom concrete floor (foundation) – 510 m2

3. RESULTS OF THE CALCULATION

3.1 Accident Description

The analyzed transient was a station blackout which included the loss of both off-site and on-site AC power. The only systems available were passive safety systems: accumulators and the turbine driven AFW system. The high-pressure and the low-pressure safety injection pumps were disabled. Containment safety systems, fan coolers and sprays, were also inoperable. Following the loss of AC power, RCP seals will overheat due to non-existent cooling normally provided by the charging pumps, a break will be formed and coolant will be released from the reactor cooling system to the containment.

Reactor coolant pumps and the feedwater pumps were tripped at 0 s. At the same time the break at both RCPs was opened. Shortly afterwards, the reactor and the turbine were tripped due to the low cold leg coolant flow. Power-operated pressurizer and steam generator relief valves were disabled, as well as pressurizer heaters. Safety valves were operable, but only SG valves were actuated, since due to the LOCA conditions, primary system pressure decreased from the beginning of the transient and, thus, no overpressure on the pressurizer safety valves occurred that would lead to their opening.

Five cases were analyzed depending on the fraction of entrained corium reaching the containment atmosphere after the breach of the reactor vessel. The fraction was varied in the increments of 25%, from 0% to 100%. Dispersed corium debris would heat up the air and the structures on which it adheres making it an extra heat source in the containment, along with the mass and energy release from the primary system.

Additionally, results of the “wet cavity” and the “dry cavity” calculations were compared. The cavity is separated from the containment by the water tight door. The door is closed during the normal NPP operation and only after its failure, caused by the pressure build-up during the MCCI, water could enter the cavity. The “wet cavity” model assumed no door was present from the start of the accident maximizing water inflow to the cavity and providing enhanced cooling of the corium. In the “dry cavity” model there was no connection between the cavity and the annular space surrounding it. However, some water accumulated in the cavity because of the condensation of steam released from the primary system, but its quantity was negligible.

3.2 Containment Behaviour

Containment pressures are shown in Figure 3 and containment temperatures in Figure 4. After the opening of the breaks and release of the primary coolant, the pressure will increase to 120 kPa and remain more or less constant during the next three hours. In the meantime, the reactor core will overheat and melt due to the absence of the active safety injection systems. Relocation of the molten material to the RPV lower head will cause the heat-up and breach of the reactor vessel, and release of the corium into the containment cavity.

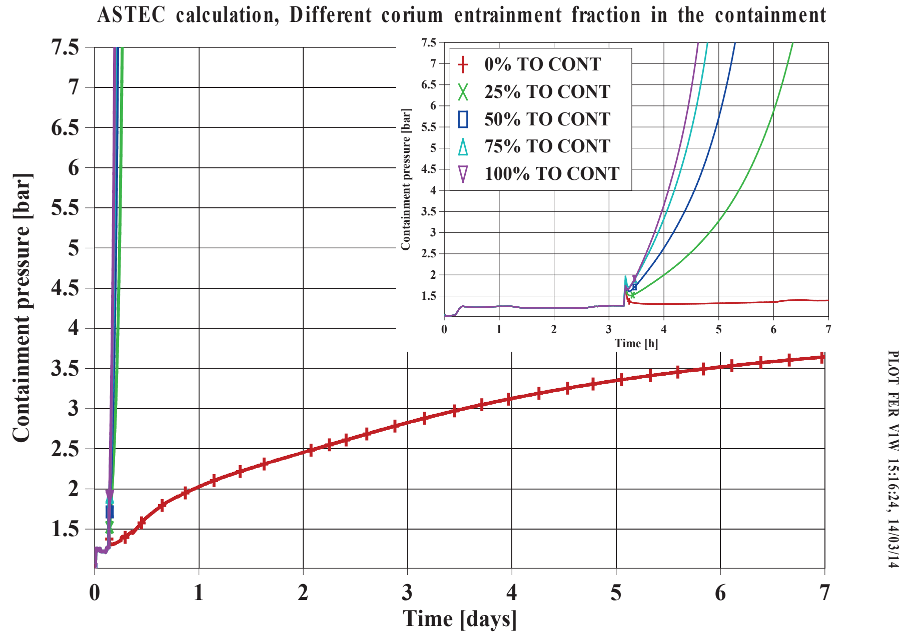

Figure 3. Containment pressure for different corium entrainment fractions

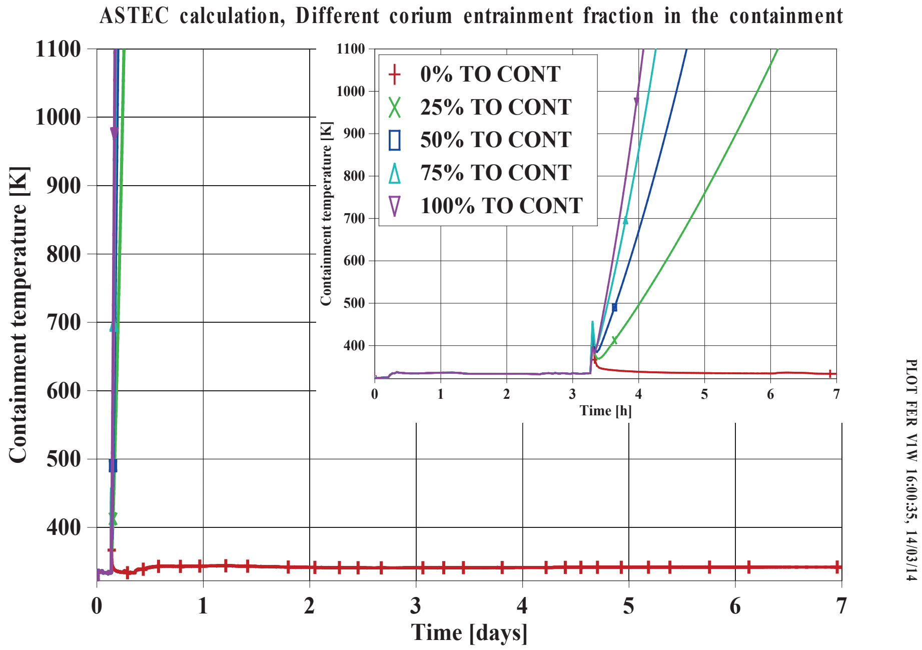

Figure 4. Containment temperature for different corium entrainment fractions

Discharge of the molten corium is followed by the blow-down of primary circuit gases. If the blow-down is significant enough; the primary pressure at the time of the vessel failure is around 5 MPa; it may cause entrainment of the corium debris by the hot gases flowing from the cavity to the other compartments of the containment. Dispersal of the corium as finely particulate droplets may potentially result in a rapid heating and pressurization (direct containment heating). Only a fraction of the corium will reach the containment depending on the user's input. Five cases were analyzed with the fractions being set to 0%, 25%, 50%, 75% and 100%. When no DCH was taken into account, a steady pressure increase was calculated with the containment temperature being almost constant at 70 °C. The pressure rise was attributed to accumulation of incondensable gases released during the process of the molten corium concrete interaction. Decay heat of the fission products inside the corium was efficiently removed by conduction through the containment floor and by convection into the environment.

Corium entrainment led to fast temperature and pressure increase. In less than three hour time, for the case with the minimum fraction of dispersed corium, the containment pressure reached 7.5 bar, the value for which the containment failure probability is 50% according to the NPP Krško containment fragility curve. Heat transfer coefficient from corium droplets to the atmosphere was 500 W/m^{2}K as recommended by the ASTEC development team and the heat transfer was enhanced by assuming a rapid thermal equilibrium between the droplets in the containment atmosphere which is a default option in the code [3].

In the case with no corium discharge in the containment, as already mentioned, the temperature was constant, but the pressure rose from 1.2 bar to 3.6 bar. The main reason was production of carbon dioxide during the MCCI process. Figure 5 shows partial pressures of gases in the containment. A direct influence of the CO_2 partial pressure on the total containment pressure can be observed. Immediately, after the MCCI started, hydrogen and carbon monoxide were produced as a result of oxidation of metals contained in the corium. Their accumulation and oxidation heat release were the reasons for the pressure and temperature increase in the first 11 hours. After all metals had oxidized, only CO_2 was produced afterwards. There was no abruptly pressure rise because no hydrogen or CO ignition was calculated to occur.

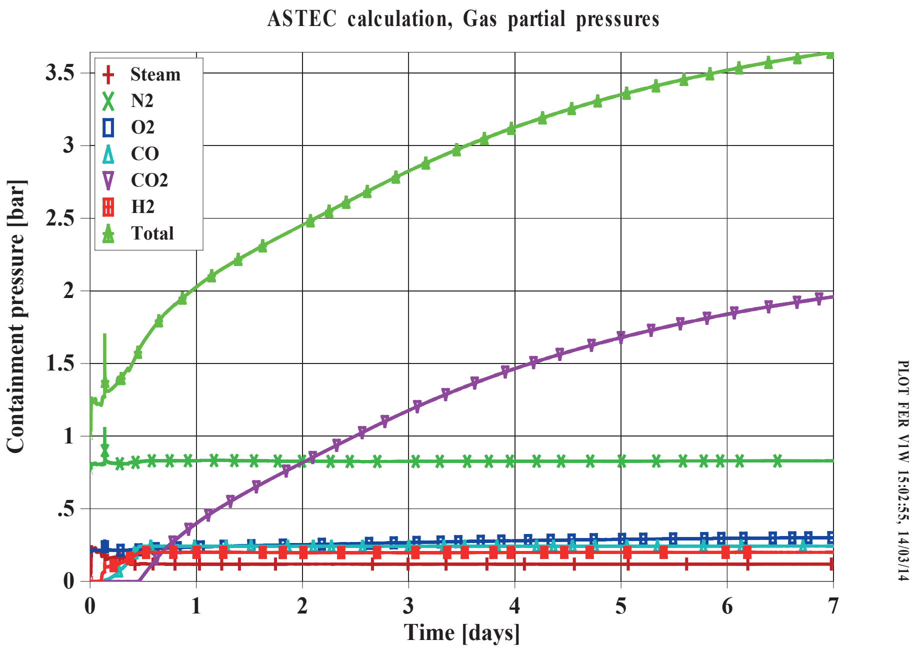

Figure 5. Gas partial pressures in the containment

Hydrogen, CO and CO_2 are products of the concrete decomposition by the molten corium. At temperatures 600–900 °C calcium carbonate is decomposed into calcium oxide and carbon dioxide [5]:

$$CaCO_3 \rightarrow CaO + CO_2$$

The reaction is endothermic, thus $CaCO_3$ absorbs energy of the radioactive decay of the fission products in the melt. The released CO_2 and steam produced by evaporation of water from the concrete will be used for the metals oxidation:

$$Zr + 2\ H_2O \rightarrow ZrO_2 + 2\ H_2$$

$$Zr + 2\ CO_2 \rightarrow ZrO_2 + 2\ CO$$

$$2\ Cr + 3\ H_2O \rightarrow Cr_2O_3 + 3\ H_2$$

$$2\ Cr + 3\ CO_2 \rightarrow Cr_2O_3 + 3\ CO$$

$$Fe + H_2O \rightarrow FeO + H_2$$

$$Fe + CO_2 \rightarrow FeO + CO$$

Oxidation of zirconium and chromium are exothermic reactions, while iron oxidation is an endothermic reaction [5]. The code assumes that all CO_2 is going to be spent on metals oxidation, so as long as there are free metal atoms, hydrogen and CO are released in the containment, but no CO_2. Afterwards, calcium carbonate decomposition will be the only reaction associated with release of incondensable gases (CO_2). This becomes apparent when gas masses are compared (Figure 6). Up to 11 hours of the transient, metals oxidation process generated H_2 and CO, while the mass of CO_2 was 0 kg. Metals consumption after 11 hours marked the start of CO_2 release and termination of H_2 and CO generation.

The final amount of gases produced during the accident is shown in Table I. Since CO_2 starts to be generated later in the accident, its mass is different than 0 kg only in the case with no corium entrainment. Hydrogen and CO masses depend on the calculation time and mass of reacted corium. The case with 100% corium entrainment fraction results with the lowest amount of hydrogen and carbon monoxide. The latter is only 0.2 kg because for CO to be produced, there has to be CO_2 available which is, on the other hand, mainly produced by the concrete dissolution. Assuming complete corium dispersal out of the reactor cavity, the temperature necessary for $CaCO_3$ decomposition will not be achieved and, thus, no CO_2 will be released. The amount of hydrogen is 8 kg higher than the mass generated during the oxidation of the reactor core in the in-vessel phase of the accident (206.6 kg). That additional hydrogen was mainly produced during the oxidation reaction of corium debris scattered throughout the containment with the steam already present in the containment atmosphere. In short, as the fraction of entrained corium increases, the MCCI process becomes less important and CO and CO_2 production decreases. Positive consequence of that is not only the pressure reduction but also the fact that CO is an explosive gas. Hydrogen is still being generated, but now, beside the MCCI, also during the oxidation of metals in the corium particles. That reaction is less significant than the corium oxidation in the reactor cavity due to a smaller amount of accumulated heat. The shortcoming of the corium entrainment is the process of direct containment heating which results in a much faster containment pressurization.

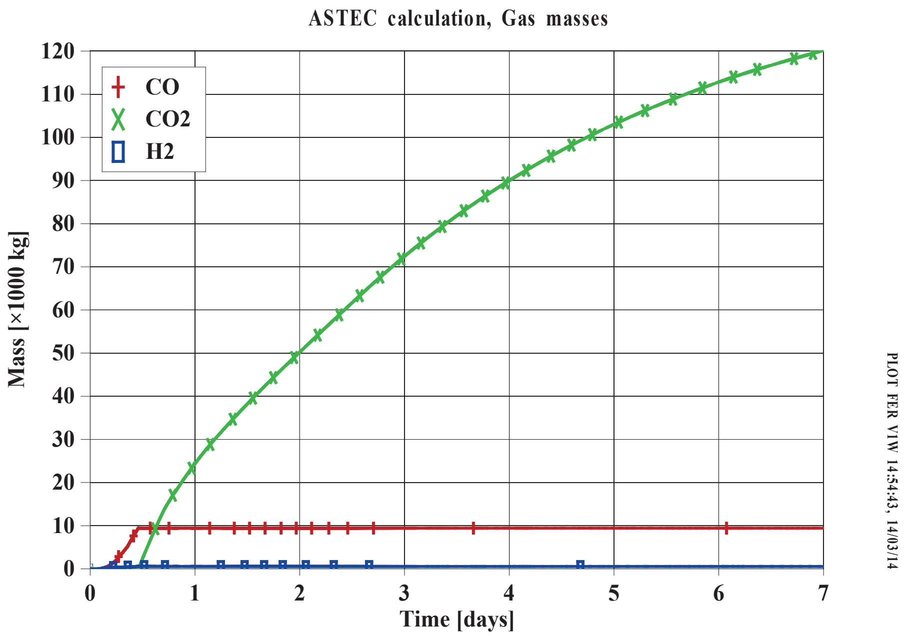

Figure 6. Mass of incondensable gases in the containment

Table I. Final amount of incondensable gases

Case	Hydrogen [kg]	Carbon monoxide [kg]	Carbon dioxide [kg]
0%	555.3	9392	120122
25%	321.2	1801	0
50%	272.7	230.1	0
75%	267.9	72.7	0
100%	214.7	0.2	0

The molten corium concrete interaction will erode the concrete as shown in a sketch on Figure 7. The MCCI is preceded by the processes of corium slumping from the vessel into the cavity and the primary circuit gases blow-down which both lasted for few seconds after the RPV failure. During the slumping there was no corium fragmentation in the water present in the cavity. In the ASTEC ex-vessel modules there is no simulation of the fragmentation process. The corium jet fragmentation can at present time only be accounted for in the ICARE lower head modelling. Therefore, without the DCH that could transport corium fragments outside the cavity domain, the MCCI simulation in the ASTEC is in that case starting with the corium composition and arrangement strictly as it is when entering the cavity from the vessel during the slumping process. At the end of the slumping phase, the corium is assumed to be located on the containment bottom, completely filling the cavity floor. The spreading area is relatively large (38.2 m^2), so the initial corium thickness is less than 10 cm. Nevertheless, its potential for concrete dissolution is large enough to cause severe damage of the containment floor.

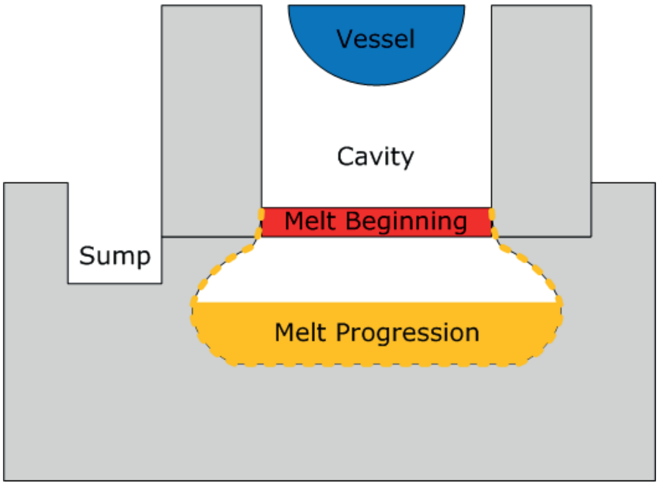

Figure 7. Cavity erosion during the MCCI

Figure 8 shows initial and final cavity temperature profiles, indicating concrete degradation during the MCCI. Maximum radial and vertical erosion depths are shown in Figure 9, while the mass of eroded concrete is shown in Figure 10. Concrete erosion is a progressive process that could not be mitigated due to continuous production of decay heat inside the melt. Hence, the mass of molten corium released from the vessel was 23.75 tons and the mass of dissolved concrete after seven days of molten corium concrete interaction reached 500 tons with the tendency to increase further. The cavity erosion was modelled to be two dimensional. The amount of liquefied concrete was calculated based on the data of the latent heat of fusion, corium-concrete phase diagrams and the concrete composition [2]. The former two data-sets and appropriate correlations are incorporated in the code package. The concrete composition was entered in the input file. Bali correlation was used to compute the heat transfer coefficient between the corium and the concrete [6].

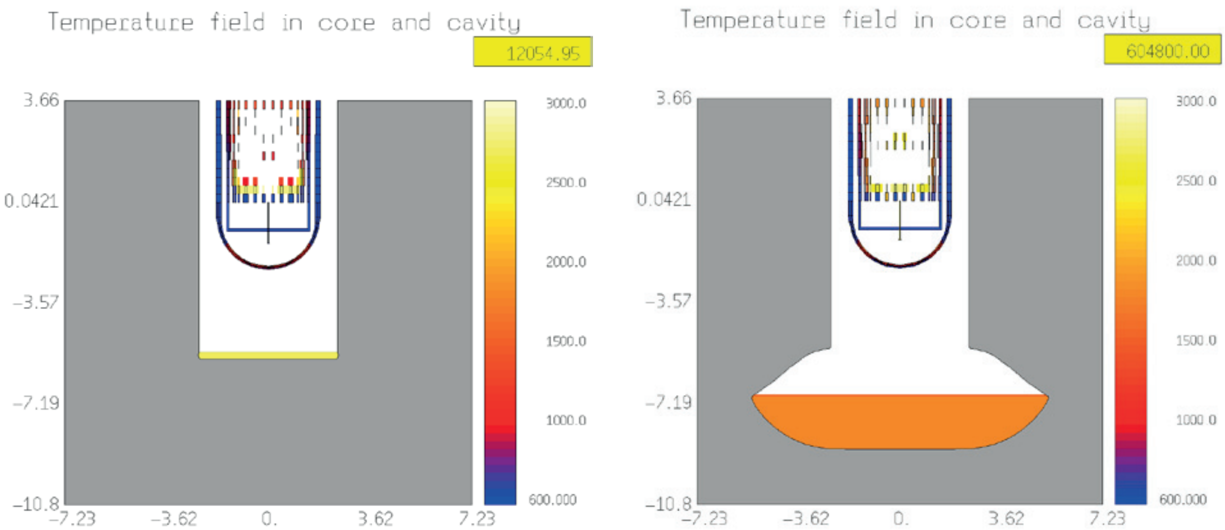

Figure 8. Initial and final cavity temperature profiles as calculated by ASTEC

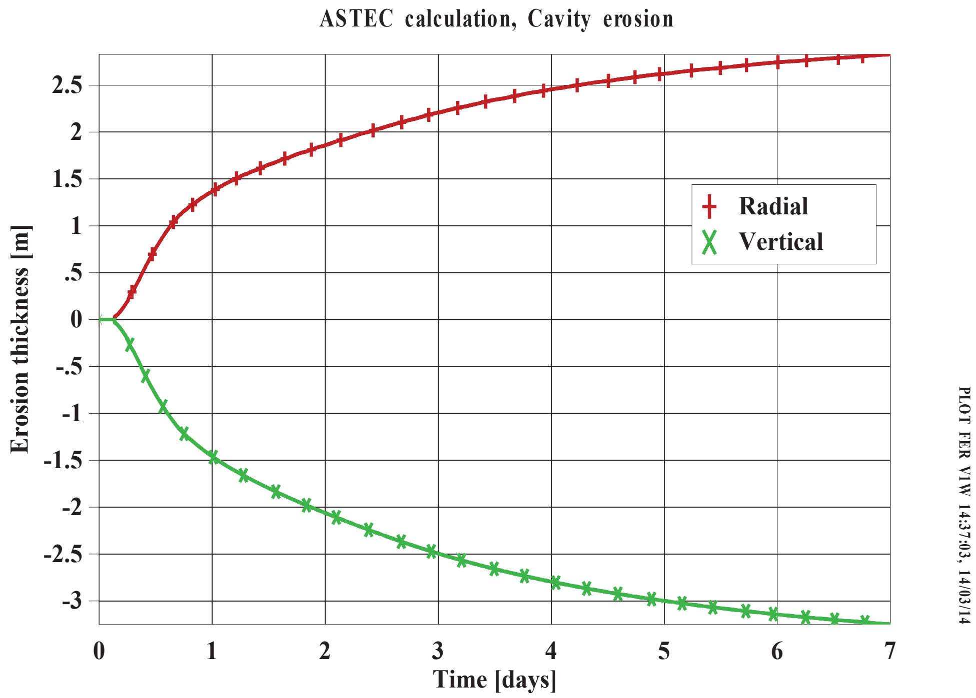

Figure 9. Cavity erosion depths in radial and vertical directions

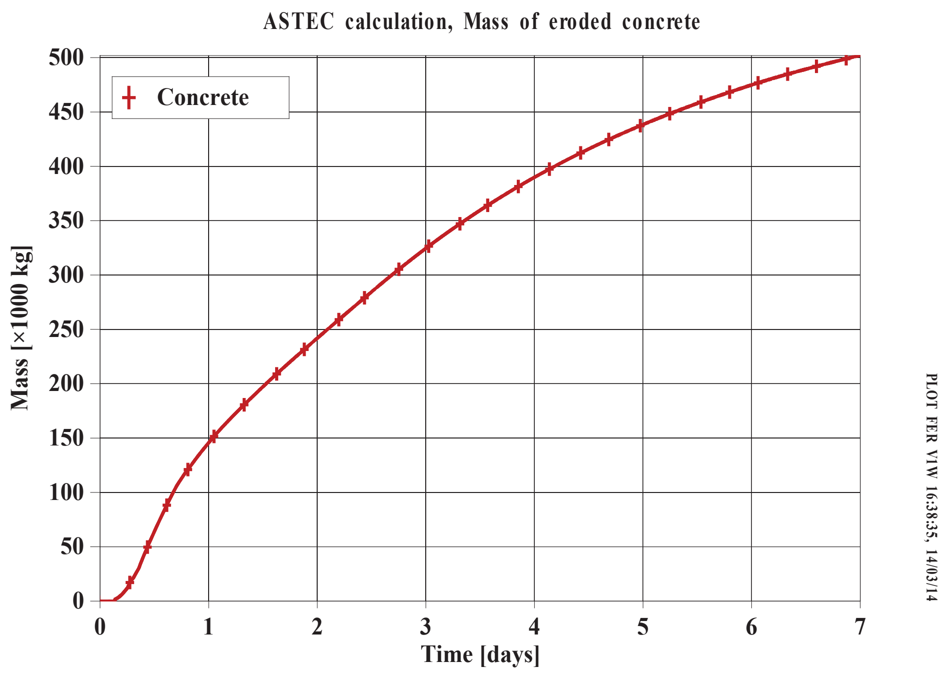

Figure 10. Mass of eroded concrete

3.3 Influence of Cavity Flooding

Previous calculations were performed with the water already present in the cavity before the melt was released out of the reactor vessel. Water entered the cavity compartment through the narrow space between the lower compartment and the cavity areas. Normally, that connection does not exist because the space is closed with the water tight door preventing the leakage. The door could only be breached by the over-pressurization during, for example, the process of MCCI. A calculation with no cavity flooding was performed and its results were compared with the “wet cavity” analysis results, Figure 11 and Figure 12.

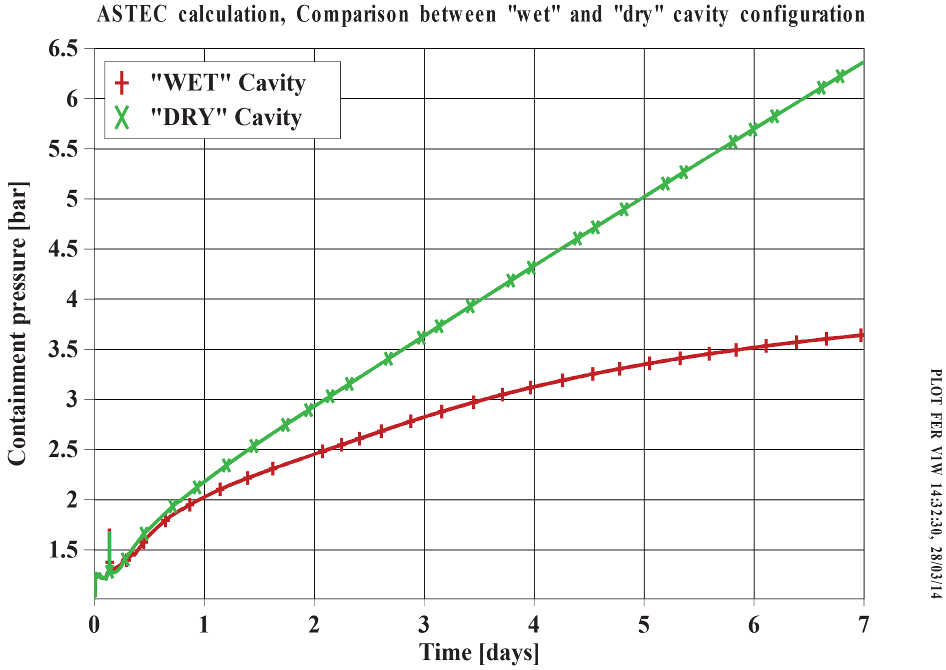

Figure 11. Containment pressure for the cases with and without the water present in the cavity

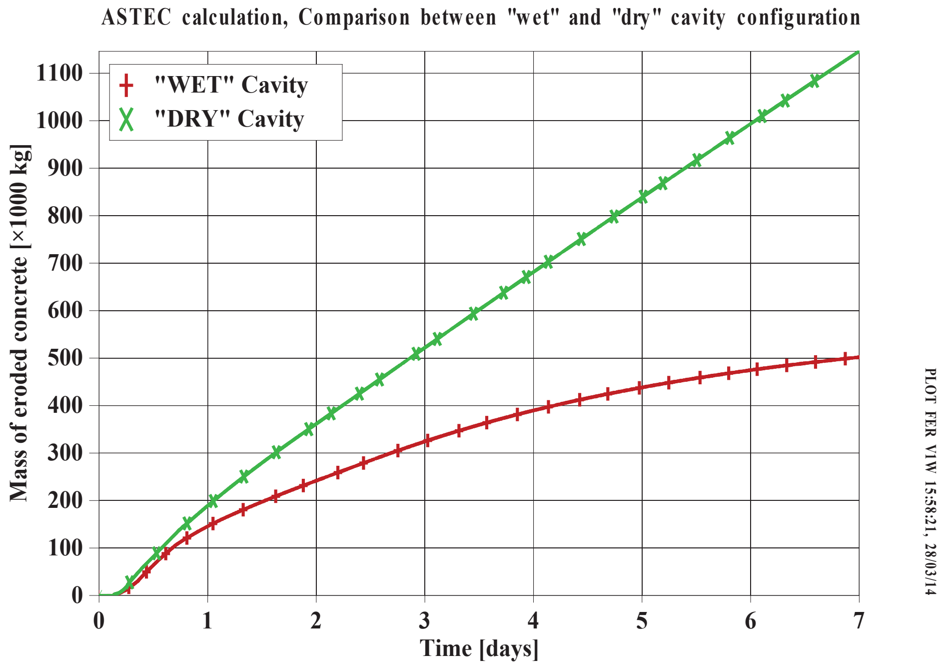

Figure 12. Mass of eroded concrete for the cases with and without the water present in the cavity

A dry cavity at the time of corium discharge from the RPV in the containment influenced latter containment behaviour. The pressure increased faster than in the case with the flooded cavity because more carbon dioxide was released during the MCCI. The molten corium concrete interaction was more intensive; more concrete was dissolved and larger quantities of H_2, CO and CO_2 were released.

The impact of the dry cavity was not as important as the DCH regarding the containment integrity. The rate of pressure rise was more than ten times higher for the DCH than for the MCCI mechanisms. The DCH was accompanied with a fast temperature increase caused by the containment atmosphere heat-up. The heat transfer from the dispersed corium to the air and steam forced the pressure to increase with the same rate as the temperature. On the other hand, there was no significant temperature increase during the MCCI. The process of concrete erosion is mainly endothermic [5] except for the initial period of metal oxidation. Decay heat inside the corium was removed by conduction through the containment foundation, while on the top of the molten material, formation of a crust altered the heat transfer to the surrounding air.

4. CONCLUSION

PWR containment behaviour during a hypothetical severe accident was analyzed with the ASTEC code. The sequence included release of the coolant from the primary system and discharge of corium after the breach of the reactor pressure vessel. The containment was modelled with ten control volumes representing real compartments such as steam generator, pressurizer, sump and cavity compartments. The largest volume was the containment dome above the elevation of the uppermost floor slab.

Containment integrity depends on the inside pressure and temperature. The initial release of steam only slightly affected the pressure. Main reasons for the containment heat-up and pressurization were the molten corium concrete interaction and the direct containment heating. During the MCCI molten corium dissolves the concrete and incondensable gases hydrogen, carbon monoxide and carbon dioxide are released. Primarily, CO_2 is responsible for the pressure rise because of its large quantity. Temperature increased by 10 °C shortly after the start of the concrete erosion due to oxidation of metals in the corium but afterwards it did not change a lot because concrete decomposition is an endothermic process. The MCCI is an undesirable severe accident event for the reason of producing flammable and explosive gases H_2 and CO. No hydrogen or CO deflagration was calculated to occur.

Molten debris dispersion in the containment atmosphere (DCH) led to rapid heat-up and pressurization. Decay heat in the melt was transferred to containment structures and walls, and also to air and steam which, due to low heat capacity, experienced fast temperature rise. The containment pressure reached the threshold value for the rupture three hours after the release of the corium in the containment.

In the case with no DCH, the containment pressure was less than the limiting pressure for more than a week, thus, providing important time window to undertake mitigating actions.

ACKNOWLEDGMENTS

The authors would like to express their gratitude to the IRSN for providing the ASTEC code and to the NPP Krško for providing the plant data.

REFERENCES

[1] P. Chatelard, N. Chikhi, L. Cloarec, O. Coindreau, P. Drai, F. Fichot, B. Ghosh, G. Guillard, “ASTEC V2 Code: ICARE Physical Modelling”, ASTEC-V2/DOC/09-04, DPAM-SEMCA-2009-148, Revision 0, 2009.

[2] F. Duval, M. Cranga, “ASTEC V2 MEDICIS MCCI Module: Theoretical Manual“, DPAM/SEMIC 2008-102, Revision 1, 2008.

[3] M. Cranga, P. Giordano, R. Passalacqua, C.Caroli, L.Walle, “ASTEC V1.3: RUPUICUV Module: Ex-vessel Corium Discharge and Corium Entrainment to Containment“, ASTEC-V1/DOC/03-19, Revision 1, 2003.

[4] C. Seropian, F. Jacq, L.Walle, “Description of the CORIUM Module of the ASTEC Code“, ASTEC-V1/DOC/04-11, Revision 0, 2004.

[5] Z.P. Bažant, M.F. Kaplan, “Concrete at High Temperatures: Material Properties and Mathematical Models”, Longman (Addison-Wesley), monograph and reference volume, 412 + xii pp., London, 1996.

[6] J.M. Bonnet, “Thermal Hydraulic Phenomena in Corium Pools for Ex-vessel Situations: The Bali Experiment”, In Proceedings of the 8th International Conference on Nuclear Engineering 2000, ICONE-8, number ICONE-8177, Baltimore, Maryland, USA, 2000.